

CHARM CONTENT OF A PHOTON AND J/ψ PHOTOPRODUCTION AT HIGH ENERGIES

V.A.Saleev

Samara State University, Samara, 443011, Russia

Abstract

A study of the J/ψ -meson production at large transverse momentum in high energy γp collisions via the charm quark excitation in a photon is presented. Based on perturbative QCD and the nonrelativistic quark model, our calculation demonstrates that the charm content of a photon may be very important for the J/ψ photoproduction at the large transverse momentum. It is shown that at HERA energies J/ψ production via the subprocess $c(\gamma)g \rightarrow J/\psi c$ dominates over the resolved photon contribution via the subprocess $g(\gamma)g \rightarrow J/\psi g$ at $p_\perp > 3$ GeV/c and over the direct photon-gluon fusion contribution at $p_\perp > 10$ GeV/c.

1 Introduction

The study of a different mechanisms of the inclusive J/ψ photoproduction on protons is of a particular importance because the process of J/ψ production via photon-gluon fusion plays a crucial role in the measurement of gluon structure function in a proton [1, 2, 3, 4]. Previous calculations of J/ψ photoproduction at large p_\perp have included direct charmonium production via photon-gluon fusion using the colour singlet model [1, 2], diffractive inelastic J/ψ production [5], resolved photon contributions via subprocesses $gg \rightarrow J/\psi g$, $gg \rightarrow \chi_{0,2} \rightarrow J/\psi \gamma$ [4] and J/ψ production from b quark decays [6]. Here we examine the diffractive-like contribution of the charm quark excitation in a photon to the J/ψ photoproduction at large p_\perp via partonic subprocess $c(\gamma)g \rightarrow J/\psi c$, where charm quarks in the initial state are not pure "intrinsic" [7] but are generated by QCD evolution of the photon structure functions (PSF) [8]. We suppose that at low Q^2 the charm content of the photon is virtually nil, but at Q^2 of order m_c^2 one has sufficient resolution to find charm quarks in photon. Note, that in the processes of the J/ψ photoproduction at large p_\perp the relevant QCD scale $Q^2 \sim M_\psi^2 + p_\perp^2 \gg m_c^2$. Our calculation is partly the same as the approach used in Ref.[9] for description of the charm quark hadroproduction and based on the fact that both the central and diffractive components of charm production can be understood in the context of perturbative QCD. Recently we have presented the results of the calculations for contributions of the intrinsic charm in the proton to the J/ψ photoproduction [10] and hadroproduction [11].

The study of a photon structure function [8] in the resolved-photon interaction at HERA energy and beyond is also very interested [12]. Usually it is supposed that at high energy in the resolved-photon interaction the gluon content of a photon is dominant. In this paper we show that in the J/ψ photoproduction at larger p_\perp via resolved-photon interaction the charm content of a photon is more important and it is may be studied experimentally using J/ψ plus open charm associated photoproduction.

2 Model

The process of the J/ψ photoproduction on a proton in the resolved-photon interaction is schematically presented in Fig. 1. We start from the lowest order in α_s amplitudes which correspond the set of Feynman diagrams in Fig. 2. As usual in potential model, the quarkonium is represented as nonrelativistic quark-antiquark bound system in singlet colour state with specified mass $M_\psi = 2m_c$ (m_c is charm quark mass) and spin-parity $J^p = 1^-$. The amplitudes for subprocess $c(\gamma)g \rightarrow J/\psi c$ can be expressed in the following form:

$$M_1 = g^3 T^c T^a T^a \bar{U}(q') \hat{\varepsilon}_g \frac{\hat{q}' - \hat{k} + m_c}{(k - q')^2 - m_c^2} \gamma^\mu \frac{\hat{P}}{(p - q)^2} \gamma_\mu U(q), \quad (1)$$

$$M_2 = g^3 T^a T^a T^c \bar{U}(q') \gamma^\mu \frac{\hat{P}}{(p + q')^2} \gamma_\mu \frac{\hat{k} + \hat{q} + m_c}{(k + q)^2 - m_c^2} \hat{\varepsilon}_g U(q), \quad (2)$$

$$M_3 = g^3 T^a T^c T^a \bar{U}(q') \gamma^\mu \frac{\hat{P}}{(q' + p)^2} \hat{\varepsilon}_g \frac{\hat{p} - \hat{k} + m_c}{(p - k)^2 - m_c^2} \gamma_\mu U(q), \quad (3)$$

$$M_4 = g^3 T^a T^c T^a \bar{U}(q') \gamma^\mu \frac{\hat{k} - \hat{p} + m_c}{(p - k)^2 - m_c^2} \varepsilon_g \frac{\hat{P}}{(p - q)^2} \gamma_\mu U(q), \quad (4)$$

$$M_5 = -ig^3 f^{bac} T^b T^a \bar{U}(q') \gamma^\rho \frac{\hat{P}}{(p + q')^2} \frac{\gamma^\sigma}{(q - p)^2} U(q) C_{\mu\sigma\rho} \varepsilon_g^\mu, \quad (5)$$

where

$$C_{\mu\sigma\rho} = (q + q')_\mu g_{\sigma\rho} - (p + k + q')_\sigma g_{\mu\rho} + (k - q + p)_\rho g_{\mu\sigma}.$$

The spin and colour properties of the $c\bar{c}$ -bound system is described using projection operator [1, 2]:

$$\hat{P} = \frac{F_c \Psi(0)}{2\sqrt{M_\psi}} \hat{\varepsilon}_J (\hat{p}_\psi + M_\psi), \quad (6)$$

where $F_c = \delta^{kr}/\sqrt{3}$, k and r are colour indexes of charm quarks, $T^a = \lambda^a/2$. The value of J/ψ wave function at the origin $\Psi(0)$ can be extracted in the lowest order of perturbative QCD from the leptonic decay width of the J/ψ :

$$\Gamma_{ee} = 4\pi e_q^2 \alpha^2 \frac{|\Psi(0)|^2}{m_c^2}. \quad (7)$$

We shall put in our calculation $\alpha_s = 0.3$, $m_c = 1.55$ GeV, $\Gamma_{ee} = 5.4$ KeV [9].

After average and sum over spins and colours of initial and final particles, we obtain the expression for square of matrix element:

$$|\bar{M}|^2 = B_{gc} \sum_{i \leq j=1}^5 C_{ij} K_{ij}(\hat{s}, \hat{t}, \hat{u}), \quad (8)$$

where

$$B_{gc} = \frac{\pi^2 \alpha_s^3 \Gamma_{ee}}{16\alpha^2 m_c},$$

$\hat{s} = (k + q)^2$, $\hat{t} = (k - q')^2$, $\hat{u} = (q - q')^2$ are usual Mandelstam variables and $\hat{s} + \hat{t} + \hat{u} = 6m^2$. The explicit analytical formula for functions K_{ij} are given in Appendix.

The appropriate colour factors are:

$$\begin{aligned}
C_{11} &= C_{22} = C_{12} = C_{21} = 64/9, \\
C_{33} &= C_{44} = C_{34} = C_{43} = 1/9, \\
C_{13} &= C_{31} = C_{14} = C_{41} = C_{23} = C_{32} = C_{24} = C_{42} = -8/9, \\
C_{15} &= C_{51} = C_{25} = C_{52} = 8, \\
C_{35} &= C_{53} = C_{45} = C_{54} = -1, \quad C_{55} = -9
\end{aligned} \tag{9}$$

The differential cross section for subprocess $c(\gamma)g \rightarrow J/\psi c$ can be written as follows:

$$\frac{d\hat{\sigma}}{d\hat{t}} = \frac{\overline{|M|^2}}{16\pi(\hat{s} - m_c^2)^2} \tag{10}$$

In the conventional parton model the measurable cross-section is obtained by folding the hard parton level cross-section with the respective parton densities:

$$\begin{aligned}
\frac{d\sigma}{d^2p_\perp dy} &= \int dx_1 \int dx_2 C_\gamma(x_1, Q^2) G_p(x_2, Q^2) \\
&\frac{d\hat{\sigma}}{d\hat{t}}(cg \rightarrow J/\psi c) \frac{x_1 x_2 s}{\pi} \delta(\hat{s} + \hat{t} + \hat{u} - M_\psi^2 - 2m_c^2).
\end{aligned} \tag{11}$$

Here: $\hat{s} = x_1 x_2 s + m_c^2$, $\hat{t} = M_\psi^2 + m_c^2 - x_1 \sqrt{s} M_\perp \exp(-y^*)$, $\hat{u} = M_\psi^2 - x_2 \sqrt{s} M_\perp \exp(y^*)$, $M_\perp = \sqrt{M_\psi^2 + p_\perp^2}$, where y is the J/ψ rapidity in c.m.s., p_\perp is the J/ψ transverse momentum, $G_p(x_2, Q^2)$ is the gluon distribution function in a proton, at the scale $Q^2 = M_\perp^2$, $C_\gamma(x_1, Q^2)$ is the charm quark distribution function in a photon, s is the square of a total energy of colliding particles in the γp center of mass reference frame. We use in calculations LO GRV [14] parameterization for $G_p(x_2, Q^2)$ structure function. The input charm quark distribution $C_\gamma(x_1, Q^2)$ demands the more careful consideration.

In all QCD motivated parton distributions of the photon [15] heavy quarks are considered as an intrinsic massless parton whose distribution is generated according to the Altarelli–Parisi equations. In spite of the fact that in the process of the J/ψ production at large p_\perp the relevant scale $Q^2 \gg m_c^2$ and a resummation procedure of the perturbation series $(\alpha_s \log(Q^2/m_c^2))^n$ is valid, we don't use these parameterizations taking into account that our consideration based on the full massive subprocesses. As it was shown in Ref. [16], the concept of the massless intrinsic heavy quark distributions yield a overestimated result for heavy quarks production at high energies. That is why more grounded to use "hard" phenomenological parameterization based on the vector-meson-dominance (VMD) model. In the approach of VMD model the c-quark PSF is presented via the charm quark distribution function of the J/ψ meson:

$$C_\gamma(x) = k \frac{4\pi\alpha}{f_\psi^2} C_\psi(x), \tag{12}$$

with $1 \leq k \leq 2$. The precise value of k clearly has to be extracted from experiment. Similar to Ref. [17], where the photoproduction of charm hadrons in VMD model has been discussed, we use for distribution charm quark in J/ψ -meson the simple scaling parameterization

$$C_\psi(x) = 49.8x^{1.2}(1-x)^{2.45}. \tag{13}$$

We want to note that this parameterization takes into account heavy quark mass effects [17], which are principal for our consideration.

Let us next consider the dynamical cutoff for the charm excitation processes. For the typical charm excitation diagram (Fig.2), the charm quark must receive sufficient transfer

momentum, which is necessary to excite $c\bar{c}$ pair. This implies a minimum dynamical resolution $|\hat{t}|_{min}$ for the momentum transfer \hat{t} of the $c(\gamma)g \rightarrow J/\psi c$ subprocesses. We choose $|\hat{t}|_{min} = m_c^2$, although the specification of the scale is uncertain by factors [9]. The dependence of our results from the choice of $|\hat{t}|_{min}$ will be discussed later.

3 Results and discussion

Because of the relevant QCD scale Q^2 is order of M_\perp , we consider at first p_\perp distribution of the J/ψ -mesons which are generated in γp collisions via charm excitation in the photon. Fig. 3 shows our predictions for J/ψ 's p_\perp -spectra at the energy $\sqrt{s_{\gamma p}} = 200$ GeV. The solid curve corresponds to the contribution of the photon-gluon fusion mechanism. The short-dashed curves are contributions of the charm excitation subprocesses at different choice of dynamical cutoff: upper curve corresponds to $|\hat{t}|_{min} = m_c^2$, lower curve - $|\hat{t}|_{min} = 4m_c^2$. The long-dashed curve is the contribution of the resolved photon interaction via subprocess $g(\gamma)g \rightarrow J/\psi g$. We can see that the result of calculation for charm excitation mechanism is independent from $|\hat{t}|_{min}$ at $p_\perp > 5$ GeV/c. But in low p_\perp region one has strong suppression of the p_\perp -spectrum versus $|\hat{t}|_{min}$. So, our predictions, based on the charm excitation mechanism, are realistic for large p_\perp where $|\hat{t}|_{min}$ cutoff influence is absent.

Fig. 3 demonstrates the crossing of the solid and short-dashed curves at $p_\perp = 10$ GeV/c and at large $p_\perp > 10$ GeV/c the charm excitation mechanism dominates over the direct photon-gluon fusion. The contribution of the resolved photon interaction via subprocess $g(\gamma)g \rightarrow J/\psi g$ is bigger the contribution of the $c(\gamma)g \rightarrow J/\psi c$ subprocess only at $p_\perp < 2$ GeV/c. The rapidity distribution, which are presented in Fig. 4, also shows us the sufficient role of the charm excitation process in the J/ψ photoproduction at large p_\perp . We see that the contribution of this one in the J/ψ 's rapidity spectrum at $p_\perp > 7$ GeV/c is dominant in the wide rapidity region $-0.7 < y^* < 2.0$.

In the Fig. 5 the results of calculation for the total cross section of the J/ψ photoproduction at $p_\perp > 7$ GeV/c versus $\sqrt{s_{\gamma p}}$ are presented. The contribution of the subprocess $c(\gamma)g \rightarrow J/\psi c$, which is independent of the dynamical cutoff at large p_\perp , rapidly grows beginning with $\sqrt{s_{\gamma p}} = 40$ GeV and at $\sqrt{s_{\gamma p}} = 200$ GeV one has $\sigma(\gamma g \rightarrow J/\psi g)/\sigma(c(\gamma)g \rightarrow J/\psi c) \approx 1.8$. At the energies $\sqrt{s_{\gamma p}} > 200$ GeV the behaviour of the total cross sections both for the photon-gluon fusion as for the charm excitation diagrams are the same and to be conditioned by the gluon distribution function in the proton. The contribution of the resolved photon interaction via subprocess $g(\gamma)g \rightarrow J/\psi g$ in the total cross section at large p_\perp is two order of magnitude smaller the contributions of the discussed above mechanisms.

Note, that we don't take into consideration so-called K -factor which is needed as usual for normalization of the leading order QCD predictions and experimental data. In the present paper we accurately predict only relative contributions of the different J/ψ production mechanism at large p_\perp . The discussed here J/ψ photoproduction mechanism via the charm quark excitation can be used also for prediction of the open charm production rates in γp collisions at HERA energy and beyond [18].

Acknowledgements.

Author thank A. Likhoded and A. Martynenko for useful discussions. This research was supported by the Russian Foundation of Basic Research (Grant 93-02-3545) and by State Committee on High Education of Russian Federation (Grant 94-6.7-2015).

References

- [1] R. Baier, R. Ruckl: Nucl.Phys.B218 (1983) 289; B20 (1982) 1.
- [2] E.L. Berger, D. Jones: Phys.Rev.D23 (1981) 1521;
- [3] A.D. Martin, C.-K. Ng, W.J. Stirling: Phys.Lett.B191 (1987) 200.
- [4] H. Jung, G.A. Schuler, J. Terron: Int.J.Mod.Phys.A32 (1992) 7955.
- [5] G.A. Schuler, J. Terron: DESY preprint 92-017 (1992).
- [6] Z. Kunszt : Phys.Lett. B207 (1988) 103.
- [7] S.J.Brodsky, P.Hoyer, C.Peterson, N.Sakai: Phys.Lett. 93B (1980) 451.
- [8] E. Witten: Nucl.Phys.B120 (1977) 189;
Ch. Berger, W. Wagner: Phys.Rep.146 (1987) 1.
- [9] V.Barger, F.Halzen, W.Y.Keung: Phys.Rev. D25 (1982) 112.
- [10] V.A. Saleev: Mod.Phys.Lett.A12 (1994) 1083.
- [11] A.P. Martynenko, V.A. Saleev: Phys.Lett. B343 (1995) 381.
- [12] W. Buchmuller, G. Ingelman: 1992 Physics at HERA, Proc. Workshop 1991 (DESY).
- [13] Rewiew of Particle Properties: Phys.Rev.D45 (1992).
- [14] M.Gluck, E.Reya, A.Vogt: Z.Phys. C53 (1992) 127.
- [15] M. Drees, K. Grassie: Z.Phys. C28 (1985) 451. M.Gluck, E.Reya, A.Vogt: Phys.Rev. D45 (1992) 3986; D46 (1992) 1973; D. Duke, J.Owens: Phys.Rev. D26 (1982) 1600; H. Abramowicz, K. Charcula, A. Levy : Preprint DESY 91-069, 1991.
- [16] M.Gluck, E.Reya, M.Stratman: Nucl.Phys. B422 (1994) 37.
- [17] V.G. Kartvelishvili, A.K. Likhoded, V.A. Petrov: Phys.Lett.B (1978) 615;
A.K. Likhoded, S.R. Slabospitsky, A.N. Tolstenkov: Yad.Fiz.38 (1982) 1240.
- [18] M.Derrick et al. (ZEUS Coll.): Preprint DESY 95-013, 1995.

Figure captions.

1. The J/ψ photoproduction in resolved-photon interaction.
2. Diagrams used to describe the partonic subprocess $c(\gamma)g \rightarrow J/\psi c$.
3. The p_\perp distribution for J/ψ photoproduction at $\sqrt{s_{\gamma p}} = 200$ GeV and all y^* . The solid curve is the direct photon-gluon fusion contribution. The long-dashed curve is the resolved photon contribution via the $g(\gamma)g \rightarrow J/\psi g$ subprocess. The short-dashed curves are the contribution of the charm quark excitation in the photon, the upper curve corresponds to $|\hat{t}|_{min} = m_c^2$ and the lower curve corresponds to $|\hat{t}|_{min} = 4m_c^2$.
4. The y^* distribution for the J/ψ photoproduction at $\sqrt{s_{\gamma p}} = 200$ GeV and $p_\perp > 7$ GeV/c. Notation as in Fig. 3.
5. The total cross section for the J/ψ photoproduction at $p_\perp > 7$ GeV/c versus $\sqrt{s_{\gamma p}}$. Notation as in Fig. 3.

Appendix.

$$\tilde{t} = \hat{t}/m^2, \quad \tilde{u} = \hat{u}/m^2, \quad \tilde{s} = \hat{s}/m^2$$

$$K_{11} = -4(2\tilde{s}\tilde{t} - 2\tilde{s} + \tilde{t}^2\tilde{u} - 4\tilde{t}^2 - 8\tilde{t}\tilde{u} + 14\tilde{t} + 7\tilde{u} - 106)/(\tilde{t} - 1)^4 \quad (14)$$

$$\begin{aligned} K_{12} = & \frac{4(\tilde{s}^3 - \tilde{s}^2\tilde{t} - 6\tilde{s}^2 - \tilde{s}\tilde{t}^2 - 2\tilde{s}\tilde{t}\tilde{u} + 16\tilde{s}\tilde{t} - \tilde{s}\tilde{u}^2 + 8\tilde{s}\tilde{u} - 28\tilde{s} + \tilde{t}^3 - 6\tilde{t}^2 - \tilde{t}\tilde{u}^2 + 8\tilde{t}\tilde{u} - 28\tilde{t} + 4\tilde{u}^2 - 126\tilde{u} + 276)}{((\tilde{s} - 1)^2(\tilde{t} - 1)^2)} \end{aligned} \quad (15)$$

$$\begin{aligned} K_{13} = & \frac{8(\tilde{s}^2\tilde{t} + \tilde{s}^2 + 2\tilde{s}\tilde{t}^2 + \tilde{s}\tilde{t}\tilde{u} - 22\tilde{s}\tilde{t} + 7\tilde{s}\tilde{u} + 16\tilde{s} + 2\tilde{t}^2\tilde{u} - 24\tilde{t}^2 - 11\tilde{t}\tilde{u} + 217\tilde{t} - 2\tilde{u}^2 + 41\tilde{u} - 511)}{((\tilde{s} - 1)(\tilde{t} - 1)^2(\tilde{u} - 4))} \end{aligned} \quad (16)$$

$$\begin{aligned} K_{14} = & \frac{-8(\tilde{s}^3 + \tilde{s}^2\tilde{t} - 18\tilde{s}^2 + \tilde{s}\tilde{t}^2 + \tilde{s}\tilde{t}\tilde{u} - 16\tilde{s}\tilde{t} - \tilde{s}\tilde{u}^2 - 3\tilde{s}\tilde{u} + 166\tilde{s} - 11\tilde{t}^2 - 5\tilde{t}\tilde{u} + 115\tilde{t} + 13\tilde{u}^2 - 65\tilde{u} - 335)}{((\tilde{t} - 1)^3(\tilde{u} - 4))} \end{aligned} \quad (17)$$

$$K_{22} = -4(\tilde{s}^2\tilde{u} - 4\tilde{s}^2 + 2\tilde{s}\tilde{t} - 8\tilde{s}\tilde{u} + 14\tilde{s} - 2\tilde{t} + 7\tilde{u} - 106)/(\tilde{s}^4 - 1)^4 \quad (18)$$

$$\begin{aligned} K_{23} = & \frac{-4(\tilde{s}^2\tilde{t} - 11\tilde{s}^2 + \tilde{s}\tilde{t}^2 + \tilde{s}\tilde{t}\tilde{u} - 16\tilde{s}\tilde{t} - 5\tilde{s}\tilde{u} + 115\tilde{s} + \tilde{t}^3 - 18\tilde{t}^2 - \tilde{t}\tilde{u}^2 - 3\tilde{t}\tilde{u} + 166\tilde{t} + 13\tilde{u}^2 - 65\tilde{u} - 335)}{((\tilde{s} - 1)^3(\tilde{u} - 4))} \end{aligned} \quad (19)$$

$$\begin{aligned} K_{24} = & \frac{8(2\tilde{s}^2\tilde{t} + 2\tilde{s}^2\tilde{u} - 24\tilde{s}^2 + \tilde{s}\tilde{t}^2 + \tilde{s}\tilde{t}\tilde{u} - 22\tilde{s}\tilde{t} - 11\tilde{s}\tilde{u} + 217\tilde{s} + \tilde{t}^2 + 7\tilde{t}\tilde{u} + 16\tilde{t} - 2\tilde{u}^2 + 41\tilde{u} - 511)}{((\tilde{s} - 1)^2(\tilde{t} - 1)(\tilde{u} - 4))} \end{aligned} \quad (20)$$

$$\begin{aligned} K_{33} = & \frac{-16(2\tilde{s}^2 + 2\tilde{s}\tilde{t} + 6\tilde{s}\tilde{u} - 46\tilde{s} + \tilde{t}^2\tilde{u} - 10\tilde{t}^2 - 4\tilde{t}\tilde{u} + 74\tilde{t} + 2\tilde{u}^3 - 22\tilde{u}^2 + 53\tilde{u} - 118)}{((\tilde{s} - 1)^2(\tilde{u}^2 - 4)^2)} \end{aligned} \quad (21)$$

$$\begin{aligned} K_{34} = & \frac{-16(2\tilde{s}^2 + \tilde{s}\tilde{t} - 11\tilde{s} + \tilde{t}^2 + 2\tilde{t}\tilde{u} - 19\tilde{t} + \tilde{u}^3 - 9\tilde{u}^2 + 28\tilde{u} + 11)}{((\tilde{s} - 1)(\tilde{t} - 1)(\tilde{u}^2 - 4)^2)} \end{aligned} \quad (22)$$

$$\begin{aligned} K_{44} = & \frac{-16(\tilde{s}^2\tilde{u} - 10\tilde{s}^2 + 2\tilde{s}\tilde{t} - 4\tilde{s}\tilde{u} + 74\tilde{s} + 2\tilde{t}^2 + 6\tilde{t}\tilde{u} - 46\tilde{t} + 2\tilde{u}^3 - 22\tilde{u}^2 + 53\tilde{u} - 118)}{((\tilde{t} - 1)2(\tilde{u}^2 - 4)^2)} \end{aligned} \quad (23)$$

$$\begin{aligned} K_{55} = & \frac{4(\tilde{s}^3 - \tilde{s}^2\tilde{t} + \tilde{s}^2\tilde{u} - 14\tilde{s}^2 - \tilde{s}\tilde{t}^2 + 2\tilde{s}\tilde{t}\tilde{u} + 20\tilde{s}\tilde{t} - \tilde{s}\tilde{u}^2 - 8\tilde{s}\tilde{u} + 40\tilde{s} + \tilde{t}^3 + \tilde{t}^2\tilde{u} - 14\tilde{t}^2 - \tilde{t}\tilde{u}^2 - 8\tilde{t}\tilde{u} + 40\tilde{t} + 2\tilde{u}^3 + 4\tilde{u}^2 - 4\tilde{u} - 168)}{((\tilde{s} - 1)^2(\tilde{t} - 1)^2)} \end{aligned} \quad (24)$$

$$\begin{aligned}
K_{51} = & \frac{4(s2^3 + \tilde{s}^2\tilde{t} - 20\tilde{s}^2 - \tilde{s}\tilde{t}^2 + 2\tilde{s}\tilde{t}\tilde{u} - 12\tilde{s}\tilde{t} - \tilde{s}\tilde{u}^2 - 4\tilde{s}\tilde{u} + 168\tilde{s} - \tilde{t}^3 - 2\tilde{t}^2\tilde{u} + 24\tilde{t}^2 + \tilde{t}\tilde{u}^2 - 12\tilde{t}\tilde{u} - 88\tilde{t} + 14\tilde{u}^2 - 232)}{((\tilde{s} - 1)(\tilde{t} - 1)^3)} \tag{25}
\end{aligned}$$

$$\begin{aligned}
K_{52} = & \frac{-4(\tilde{s}^3 + \tilde{s}^2\tilde{t} + 2\tilde{s}^2\tilde{u} - 24\tilde{s}^2 - \tilde{s}\tilde{t}^2 - 2\tilde{s}\tilde{t}\tilde{u} + 12\tilde{s}\tilde{t} - \tilde{s}\tilde{u}^2 + 12\tilde{s}\tilde{u} + 88\tilde{s} - \tilde{t}^3 + 20\tilde{t}^2 + \tilde{t}\tilde{u}^2 + 4\tilde{t}\tilde{u} - 168\tilde{t} - 14\tilde{u}^2 + 232)}{((\tilde{s} - 1)^3(\tilde{t} - 1))} \tag{26}
\end{aligned}$$

$$\begin{aligned}
K_{53} = & \frac{8(4\tilde{s}^2 - \tilde{s}\tilde{t}^2 + 22\tilde{s}\tilde{t} + 10\tilde{s}\tilde{u} - 117\tilde{s} + \tilde{t}^3 + 2\tilde{t}^2\tilde{u} - 26\tilde{t}^2 - \tilde{t}\tilde{u}^2 + 2\tilde{t}\tilde{u} + 69\tilde{t} + 4\tilde{u}^3 - 29\tilde{u}^2 + 34\tilde{u} + 80)}{((\tilde{s} - 1)^2(\tilde{t} - 1)(\tilde{u} - 4))} \tag{27}
\end{aligned}$$

$$\begin{aligned}
K_{54} = & \frac{8(\tilde{s}^3 - \tilde{s}^2\tilde{t} + 2\tilde{s}^2\tilde{u} - 26\tilde{s}^2 + 22\tilde{s}\tilde{t} - \tilde{s}\tilde{u}^2 + 2\tilde{s}\tilde{u} + 69\tilde{s} + 4\tilde{t}^2 + 10\tilde{t}\tilde{u} - 117\tilde{t} + 4\tilde{u}^3 - 29\tilde{u}^2 + 34\tilde{u} + 80)}{((\tilde{s} - 1)(\tilde{t} - 1)^2(\tilde{u} - 4))} \tag{28}
\end{aligned}$$

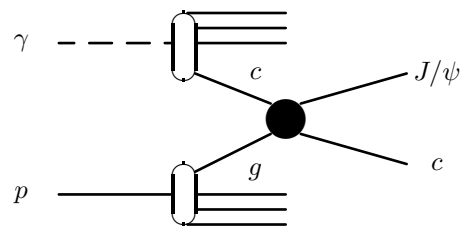


Fig.1

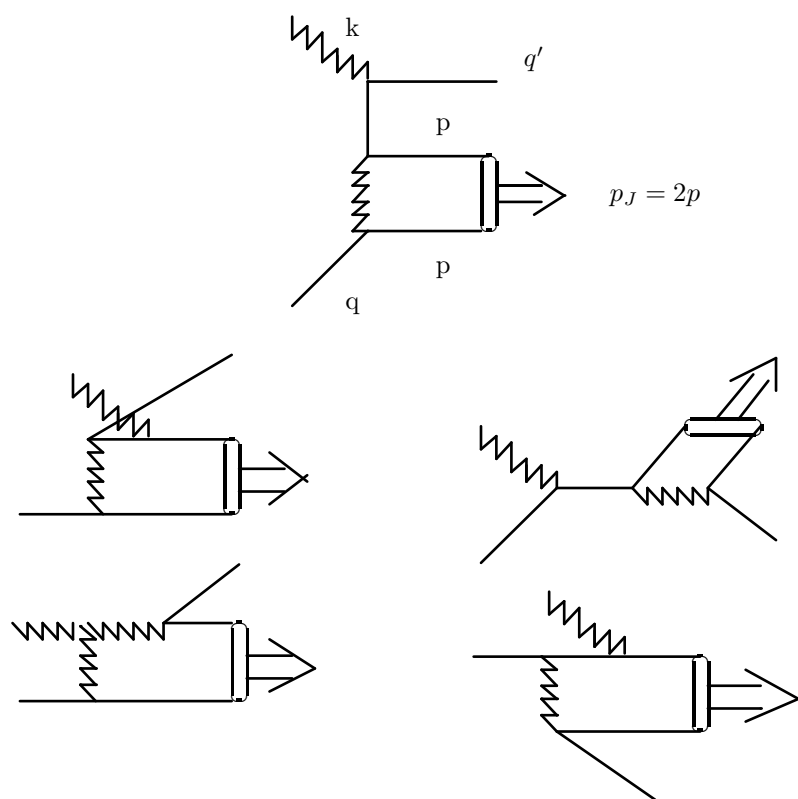


Fig. 2